
STRUCTURED MATRIX SCALING FOR MULTI-CLASS CALIBRATION

Eugène Berta^{*1,2}, David Holzmüller¹, Michael I. Jordan^{1,3}, and Francis Bach^{1,2}

¹INRIA

²Ecole Normale Supérieure, PSL Research University

³University of California, Berkeley

ABSTRACT

Post-hoc recalibration methods are widely used to ensure that classifiers provide faithful probability estimates. We argue that parametric recalibration functions based on logistic regression can be motivated from a simple theoretical setting for both binary and multiclass classification. This insight motivates the use of more expressive calibration methods beyond standard temperature scaling. For multi-class calibration however, a key challenge lies in the increasing number of parameters introduced by more complex models, often coupled with limited calibration data, which can lead to overfitting. Through extensive experiments, we demonstrate that the resulting bias-variance tradeoff can be effectively managed by structured regularization, robust preprocessing and efficient optimization. The resulting methods lead to substantial gains over existing logistic-based calibration techniques. We provide efficient and easy-to-use open-source implementations of our methods, making them an attractive alternative to common temperature, vector, and matrix scaling implementations.

1 Introduction

In multi-output classification, we aim to build a classifier f that predicts a categorical outcome $Y \in \{1, \dots, k\}$ from a feature vector $X \in \mathcal{X}$. We assume that (X, Y) are drawn independently from an underlying distribution \mathcal{D} , and we are given a dataset of feature vectors and labels $(x_i, y_i)_{1 \leq i \leq n}$ sampled from \mathcal{D} .

Many modern classifiers make continuous predictions in the probability simplex $f(X) = p \in \Delta_k$, with $\Delta_k = \{p \in [0, 1]^k \mid \mathbf{1}^\top p = 1\}$. Each component p_i represents the model's confidence that the true class is $Y = i$ and can be interpreted as the estimated probability of that event occurring. This probabilistic interpretation is valid only if the predicted probabilities align with the true underlying probabilities, a property known as *calibration*. Formally, a model f is calibrated if $f(X) = \mathbb{P}(Y \mid f(X))$ almost surely for $(X, Y) \sim \mathcal{D}$. When this holds, the prediction made by f for a new observation can be understood as a categorical distribution over the possible outcomes, which makes forecasts readily interpretable.

Unfortunately, classifiers trained on finite data, even with proper losses like cross-entropy, often exhibit significant miscalibration (Zadrozny and Elkan, 2002; Guo et al., 2017). A common remedy is *post-hoc calibration*, where a recalibration function g is applied to the output of the initial classifier f to better align its predictions with true probabilities. This is typically done by specifying a parametric model g_θ and finding parameters θ that minimize a loss function on a reserved calibration set:

$$\min_{\theta} \frac{1}{n_{\text{cal}}} \sum_{i=1}^{n_{\text{cal}}} \ell(g_\theta \circ f(x_i), y_i).$$

Critically, calibration data is often scarce, with $n_{\text{cal}} \ll n$, as we generally prefer to use all of the available data to train the classifier f . Thus, a fundamental tradeoff arises that is analogous to bias-variance tradeoffs in regression: an overly simple g_θ may be insufficient to correct the miscalibration, while with an overly complex model one risks overfitting the calibration set, potentially degrading both calibration and predictive performance. The required complexity of g_θ depends on both the amount of calibration data available and the nature of the miscalibration itself.

^{*}eugene.berta@inria.fr

A gap between theory and practice. To understand the fundamental nature of this tradeoff, we begin by analyzing an idealized setting. Consider in particular a binary classification problem with Gaussian class-conditional data; that is, $\mathbb{P}(X | Y = 0)$ and $\mathbb{P}(X | Y = 1)$ are both normally distributed with different means and variances. Consider a logistic regression classifier, $f(X) = \sigma(w^\top X)$, where $\sigma(z) = (1 + e^{-z})^{-1}$ denotes the sigmoid function. Surprisingly, even in this simple scenario the optimal recalibration function is *quadratic* in the logit:

$$\mathbb{P}(Y = +1 | f(X) = s) = \sigma(a\sigma^{-1}(s)^2 + b\sigma^{-1}(s) + c),$$

where $\sigma^{-1}(s) = \log \frac{s}{1-s}$ is the logit function (see Appendix A for the full derivation). In contrast, widely used methods such as temperature scaling (Guo et al., 2017)

$$g_b(s) = \sigma(b\sigma^{-1}(s)),$$

or Beta calibration (Kull et al., 2017)

$$g_{b,c}(s) = \sigma(b\sigma^{-1}(s) + c),$$

are linear or affine in the logits. Thus, even in this idealized setting, existing approaches are fundamentally inadequate for recalibrating the classifier f . In Appendix A we demonstrate through extensive experiments that post-hoc calibration quadratic in the logits outperforms the existing linear and affine methods, showing that this theoretical gap translates in practice.

This complexity gap becomes even more pronounced in the multiclass setting. Our analysis shows that logistic regression on multiclass Gaussian data requires post-hoc calibration with a quadratic softmax model (Section 2)—far more complex than the commonly used temperature or vector scaling (Guo et al., 2017). Previous attempts at using more expressive models such as matrix scaling have been hampered by overfitting (Guo et al., 2017), leading practitioners to employ simpler but potentially inadequate methods.

Our approach. We show that adequate regularization can unlock expressive calibration functions while avoiding overfitting. We propose structured regularization schemes that adapt the complexity of post-hoc calibration to the amount of calibration data—defaulting to simpler forms when data is scarce, and exploiting more expressive structures when sufficient data is available (Section 3). This approach allows us to handle diverse miscalibration patterns while remaining robust to overfitting.

To provide strong out-of-the-box performance, we select default regularization parameters by running an hyperparameter grid search, measuring recalibration performance on a large set of dataset-model pairs (Section 4). Our methods also allow for fine-tuning for specific applications. Through extensive experiments, we demonstrate that our methods yield substantial improvement in post-hoc calibration (Section 5).

Contributions. Our work makes three main contributions:

1. We provide theoretical motivation showing that even simple classification problems require calibration functions of higher complexity than commonly assumed.
2. We introduce structured regularization schemes that balance expressiveness and overfitting, enabling safe use of more powerful logistic calibration models. Thanks to carefully chosen hyperparameters, optimizers, and preprocessing, our methods are robust to various forms of miscalibration, alleviating the need for hyperparameter tuning.
3. We release efficient implementations in the `probmetrics` package (github.com/dholzmueller/probmetrics/), which provides faster and more accurate calibration out of the box than existing logistic methods, making our methods practical replacements for commonly used techniques.

2 Motivating Calibration with Logistic Regression

In the following, we denote by $S : \mathbb{R}^k \rightarrow \Delta_k$ the softmax function, $S(x)_i = \frac{\exp x_i}{\sum_{j=1}^k \exp x_j}$, and by I_k the $k \times k$ identity matrix.

We will see that we can motivate the use of multinomial logistic regression (also known as softmax regression) for post-hoc calibration from a simple setting.

Let us assume that $\mathcal{X} = \mathbb{R}^d$ and that the class-conditional distributions are multivariate normal distributions: $\forall i \in \{1, \dots, k\}, \mathbb{P}(X | Y = i) = \mathcal{N}(\mu_i, \Sigma_i)$ with mean vectors $(\mu_i)_{1 \leq i \leq k} \in \mathbb{R}^d$ and covariance matrices $(\Sigma_i)_{1 \leq i \leq k} \in \mathbb{S}_+^{d \times d}$. Define the softmax regression classifier, $f(X) = S(WX)$, where $W \in \mathbb{R}^{k \times d}$ is a weight matrix mapping the

feature vector $X \in \mathbb{R}^d$ to a logit vector $WX \in \mathbb{R}^k$. The distribution of logits WX in this case is normally distributed for each class:

$$\mathbb{P}(WX | Y = i) = \mathcal{N}(W\mu_i, W\Sigma_i W^\top).$$

In the multiclass case, a difficulty comes from the fact that the softmax function is not an injection. Indeed, for any scalar c , $S(z + c\mathbf{1}) = S(z)$. For this reason, the events $WX = z$ and $S(WX) = S(z)$ are not equivalent and (unlike in the binary case) the conditional distribution $\mathbb{P}(Y | WX)$ does not immediately give us $\mathbb{P}(Y | f(X))$.

To overcome this difficulty, we use the $k \times k$ centering matrix $C_k = I_k - \frac{1}{k}\mathbf{1}\mathbf{1}^\top$. The nullspace of C_k is exactly the invariant space of the Softmax: $\{c\mathbf{1} | c \in \mathbb{R}\}$. Consequently, for any centered vector $z \in \mathbb{R}^k$ with $C_k z = z$, the events $C_k WX = z$ and $S(WX) = S(z)$ are equivalent. For a given class i , the distribution of centered logits, $C_k WX$, is also a Gaussian: $\mathbb{P}(C_k WX | Y = i) = \mathcal{N}(C_k W\mu_i, C_k W\Sigma_i W^\top C_k^\top)$. However, C_k is not full rank, so the induced covariance matrix $C_k W\Sigma_i W^\top C_k^\top$ is singular. This means that the distribution is degenerate and has no density with respect to the k -dimensional Lebesgue measure. Fortunately, the disintegration theorem yields a well-defined density with respect to the Lebesgue measure when restricted to the $(k-1)$ -dimensional subspace of centered vectors. Denoting by Σ^+ the generalized inverse, $|\Sigma|_+$ the pseudo determinant, $m_i := C_k W\mu_i$ the class means, $\sigma_i := C_k W\Sigma_i W^\top C_k^\top$ the class covariances and π_i the class probabilities for all $i \in \{0, \dots, k\}$, the class-conditional density takes the form:

$$\mathbb{P}(C_k WX = x | Y = i) = \frac{\exp\left(-\frac{1}{2}(x - m_i)^\top \sigma_i^+ (x - m_i)\right)}{\sqrt{|2\pi\sigma_i|_+}}.$$

Applying Bayes' theorem (see Appendix B), we obtain that the conditional distribution of Y is:

$$\mathbb{P}(Y | C_k WX = x) = S(x^\top \mathbf{A}x + Bx + C),$$

where $\mathbf{A} \in \mathbb{R}^{k \times k \times k}$ is a three-dimensional array defined by $\mathbf{A}[i, :, :] = -\frac{1}{2}\sigma_i^+$ so that $(x^\top \mathbf{A}x)_i = -\frac{1}{2}x^\top \sigma_i^+ x$, where B is a matrix in $\mathbb{R}^{k \times k}$ defined by $B_i = m_i^\top \sigma_i^+$ and where C is a vector in \mathbb{R}^k defined by $C_i = -\frac{1}{2}m_i^\top \sigma_i^+ m_i + \log(\pi_i |\sigma_i|_+^{-1/2})$.

These calculations result in the following expression as a model for calibration:

$$\mathbb{P}(Y | f(X) = s) = S(S^{-1}(s)^\top \mathbf{A}S^{-1}(s) + BS^{-1}(s) + C),$$

where S^{-1} denotes the one-to-one mapping from probabilities to centered logit vectors: $S^{-1}(x) = C_k[\log(x_1), \dots, \log(x_k)]^\top$. Considering the post-hoc calibration function

$$g(x) = S(S^{-1}(x)^\top \mathbf{A}S^{-1}(x) + BS^{-1}(x) + C),$$

the same proof as the binary case (in Appendix A) allows us to conclude that $g \circ f$ is calibrated:

$$\mathbb{P}(Y | g \circ f(X) = p) = p.$$

Notice that if all class-conditional covariance matrices $(\Sigma_i)_{1 \leq i \leq k}$ are equal, the quadratic term in the softmax is constant and can thus be ignored. In this case, matrix scaling suffices for recalibration.

Remark. *In our example, the softmax function is well specified for calibration because the class-conditional logit distributions are Gaussian. However, performing post-hoc calibration with softmax regression does not correspond to assuming that the class-conditional distributions are normally distributed. There exists a wide range of distributions for which the conditional is logistic, as discussed in Jordan (1995) and Böken (2021). We refer the reader to Bishop (2006) for details on when the softmax model is well specified.*

3 Softmax Calibration Functions

The analysis in Section 2 motivates the use of a logistic model as a post-hoc calibration function. In practice however, we cannot compute coefficients \mathbf{A} , B and C directly. Real-world data are not normally distributed and the classifier need not be logistic regression, so logistic calibration is not necessarily well specified. Still, hopefully there exist coefficients of the softmax model g for which $g \circ f$ is approximately, or at least better calibrated than f . To find such coefficients, we resort to empirical risk minimization. Using our reserved calibration set, $(x_i, y_i)_{1 \leq i \leq n_{\text{cal}}}$, we solve the following optimization problem:

$$\min_g \frac{1}{n_{\text{cal}}} \sum_{i=1}^{n_{\text{cal}}} \ell(g \circ f(x_i), y_i), \tag{1}$$

where g is parametrized by the coefficients of the logistic model. ℓ is typically the logloss, which makes the problem convex and thus allows us to find the optimal coefficients easily.

In the literature, different choices based on the softmax model have been considered for g :

- Linear scaling (or temperature scaling (Guo et al., 2017)): $g(x) = S(\alpha S^{-1}(x))$, also applies in the multiclass case, g is parametrized only by a scalar coefficient $\alpha \in \mathbb{R}$.
- Vector scaling (Guo et al., 2017): $g(x) = S(\text{diag}(v)S^{-1}(x) + b)$, g is parametrized by an intercept vector $b \in \mathbb{R}^k$ and a $k \times k$ diagonal weight matrix with diagonal $v \in \mathbb{R}^k$.
- Matrix scaling (Guo et al., 2017): $g(x) = S(MS^{-1}(x) + b)$, g is parametrized by an intercept vector $b \in \mathbb{R}^k$ and a full weight matrix $M \in \mathbb{R}^{k \times k}$.
- To the best of our knowledge, the quadratic softmax model, $g(x) = S(S^{-1}(x)^\top \mathbf{Q} S^{-1}(x) + MS^{-1}(x) + b)$, with \mathbf{Q} a $k \times k \times k$ array of parameters, has not been studied in the literature. We will argue that this is an oversight.

Remark. In Section 2 we introduced S^{-1} as the one-to-one mapping between probabilities and centered logits $S^{-1}(x) = C_k[\log(x_1), \dots, \log(x_k)]^\top$. In practice previous work does not use centering and the multiclass logit function is simply $S^{-1}(x) = [\log(x_1), \dots, \log(x_k)]^\top$.

We cannot minimize the population risk $\mathbb{E}_{\mathcal{D}}[\ell(g \circ f(X), Y)]$ directly, but only an empirical estimate on the calibration set (1). In the multiclass case, our proposed calibration function g can have a large number of parameters ($k^3 + k^2 + k$ for the full quadratic model for example). The risk of overfitting to the calibration set, which can result in poor calibration but also degraded performance, thus needs to be considered carefully.

To navigate this risk, we take the point of view that post-hoc calibration is akin to solving a second probabilistic classification problem, with k classes and k features (the log probabilities), and under the constraint that the size of the calibration set n_{cal} is generally small. Well-established machine learning tools can help us strike the right balance. We note that Kull et al. (2019) provide a first example of this approach, by introducing ad hoc regularization on the intercept and off-diagonal coefficients of matrix scaling, yielding encouraging empirical results. Our approach introduces regularization from first principles, and we will demonstrate that this theoretically grounded approach can result in significant improvements.

It is already known from empirical studies that matrix scaling without regularization can lead to drastic overfitting on the calibration set (Guo et al., 2017; Kull et al., 2019). For this reason, and to keep the number of parameters reasonable, we decide not to explore a quadratic model, which leaves us with three models of increasing complexity: linear scaling (one parameter), vector scaling ($2k$ parameters) and matrix scaling ($k(k+1)$ parameters). Depending on the number of classes and the amount of data, we would like our model to adaptively choose between these different layers of complexity. In particular, we wish to build a single model that can replicate the behavior of the three models and never perform worse than any single model.

Our proposal is the following *structured matrix scaling* (SMS) calibration function:

$$g_{\text{SMS}}(x) = S((\alpha I_k + \text{diag}(v) + (\mathbf{1}\mathbf{1}^\top - I_k) \odot M)S^{-1}(x) + b),$$

where \odot denotes the element-wise or Hadamard product. Notice that we apply the off-diagonal mask $\mathbf{1}\mathbf{1}^\top - I_k$ coefficient-wise on the full matrix M so that its diagonal coefficients are inactive and there is no overlap with the effect of the linear and vector parameters α and v . More graphically, our function matches traditional softmax regression on the logits, using a weight matrix W with the following structure:

$$W = \begin{pmatrix} \alpha + v_1 & M_{1,2} & \dots & M_{1,k} \\ M_{2,1} & \alpha + v_2 & \dots & \vdots \\ \vdots & \ddots & \ddots & \vdots \\ M_{k,1} & \dots & \vdots & M_{k-1,k} \\ & \vdots & \vdots & \alpha + v_k \end{pmatrix}.$$

This hierarchical parameter structure gives us the freedom to apply different regularization strengths on different parameter groups. The linear parameter α is a global scaling parameter that applies to all classes. The diagonal vector v allows each diagonal entry to deviate from that global scaling factor. The off-diagonal parameters, $(\mathbf{1}\mathbf{1}^\top - I_k) \odot M$, allow for more complex inter-class dependencies. Finally the intercept vector b allows for class-specific intercepts. To learn the parameters of g_{SMS} , we propose solving the following convex optimization problem:

$$\min_{\alpha, b, v, M} \frac{1}{n_{\text{cal}}} \sum_{i=1}^{n_{\text{cal}}} \ell(g_{\text{SMS}}(x_i), y_i) + \lambda_b \frac{k^\rho}{n_{\text{cal}}^\tau} \|b\|_\delta + \lambda_v \frac{k^\rho}{n_{\text{cal}}^\tau} \|v\|_\delta + \lambda_M \frac{(k(k-1))^\rho}{n_{\text{cal}}^\tau} \|M\|_\delta. \quad (2)$$

We choose not to regularize α , assuming that linear scaling does not overfit. Otherwise, we apply penalties on the norm of each parameter group: the diagonal v , the off-diagonal $(\mathbf{1}\mathbf{1}^\top - I_k) \odot M$ and the intercept b . Intuitively, the number of parameters in each group (respectively k , $k(k-1)$ and k) as well as the number of calibration samples n_{cal} should have an effect on the regularization strength. Thus, we weight each penalty by $n_{\text{cal}}^{-\tau}$ and the group size to the power ρ . Finally, each group penalty has a specific weight λ_b , λ_v and λ_M . The hyperparameters of our regularization scheme are thus:

- The order δ of the norm used.
- The exponents τ, ρ used for the number of samples and the parameter group size.
- The group-specific weights λ_v , λ_M and λ_b .

Equation (2) is a softmax regression on the logits with a hierarchical regularization structure. We can also simplify by restricting our hierarchical model to a vector-scaling (SVS) model:

$$g_{\text{SVS}}(x) = S((\alpha I_k + \text{diag}(v))S^{-1}(x) + b),$$

which we fit by solving:

$$\min_{\alpha, b, v} \frac{1}{n_{\text{cal}}} \sum_{i=1}^{n_{\text{cal}}} \ell(g_{\text{SVS}}(x_i), y_i) + \lambda_b \frac{k^\rho}{n_{\text{cal}}^\tau} \|b\|_\delta + \lambda_v \frac{k^\rho}{n_{\text{cal}}^\tau} \|v\|_\delta. \quad (3)$$

The remaining issue is to select good values for the different regularization parameters that we introduced.

4 Hyperparameter Grid Search

For both SVS and SMS, we aim to find good values for the regularization parameters $\delta, \rho, \tau, \lambda_b, \lambda_v$, and λ_M . Ideally, we would like to derive a single parameter configuration that makes our algorithm robust to overfitting, while leaving room for additional complexity when enough data is available and recalibration can be improved further. Our goal is that with well-chosen parameters, our methods should outperform non-regularized linear, vector and matrix scaling, demonstrating that the correct regularization level can be selected adaptively. As a baseline, we consider setting all hyperparameters to one: $\lambda_b = \lambda_v = \lambda_M = 1, \tau = \rho = 1$.

To try to improve beyond this default choice, we employ meta-learning (Vanschoren, 2018). Using model predictions from TabRepo (Salinas and Erickson, 2024), we compare the performance of g_{SVS} and g_{SMS} for different regularization parameter configurations. In TabRepo, predictions are stored for $D = 68$ multiclass classification datasets. We use the predictions of $M = 7$ different models: logistic regression, CatBoost (Prokhorenkova et al., 2018), LightGBM (Ke et al., 2017), XGBoost (Chen and Guestrin, 2016), random forest (Breiman, 2001), and two neural nets from FastAI (Howard and Gugger, 2020) and AutoGluon (Erickson et al., 2020). For each dataset, the data is split in ten folds, and $T = 3$ separate tasks are created by using one of the first three folds as a test set. For each of the tasks, the remaining data is used for eight-fold cross-validation, and the predictions of the eight models on their respective validation folds are concatenated and provided as a validation set, which we use to fit post-hoc calibration models. This results in a total of $M \times D \times T \simeq 1400$ experiments. We first perform temperature scaling on all experiments and rank the datasets by the average test Brier score improvement obtained. We split the datasets into two groups by picking, in this sorted list, odd-indexed datasets for our grid search and even-indexed datasets to form a control group. This process ensures that the potential calibration gains are well distributed between the datasets we use for the grid search and the control group.

We then evaluate the average performance of g_{SVS} and g_{SMS} on the 34 grid search datasets, using the following grid of hyperparameters:

- The order δ of the norm used for regularization can be one of: ℓ_1 (LASSO regularization (Tibshirani, 1996)) which promotes sparsity on individual parameters, ℓ_2 (group LASSO (Yuan and Lin, 2006)) which promotes sparsity at the group level—setting the whole off-diagonal group to zero for example—and ℓ_2^2 (classical ridge regression). After experimenting with different values for δ , we observe more stable results with ridge regression, so we used this penalty for our grid search.
- Intuitively, groups with more parameters are more susceptible to exhibit overfitting, and we thus expect that number of parameters should have a positive impact on the penalty applied to the group. For example, off-diagonal parameters should be more regularized than diagonal parameters. Kull et al. (2019), on the other hand, heuristically employ an off-diagonal regularization scheme that is inversely proportional to the number of parameters. For completeness, we explore both positive and negative values for the exponent of the parameter group size ρ , and we consider the grid $\{-1, -0.5, 0, 0.5, 1\}$.

- Fewer regularization samples translates to higher risk of overfitting, so we only explore positive values for the exponent of the number of samples τ : $\{0.5, 1, 1.5, 2\}$.
- For the group specific coefficients λ_b , λ_v and λ_M , we explore continuous values in the range $[0.01, 100]$ using a logarithmic scale.

We use Optuna (Akiba et al., 2019) to optimize the hyperparameter configuration based on the average test Brier score improvement obtained on all grid search datasets ($\simeq 700$ experiments per configuration in total). We refer the interested reader to our experimental repository github.com/eugeneberta/LogisticCalibrationBenchmark for grid search details. As expected, hyperparameter configurations with positive values for ρ generally perform better than when negative values are used, contradicting the design choice of Kull et al. (2019).

We then compare the results obtained with the best hyperparameter configurations for SVS and SMS on the 34 control datasets (remaining $\simeq 700$ experiments) with our baseline hyperparameter choice $\lambda_b = \lambda_v = \lambda_M = 1$, $\tau = \rho = 1$. While the tuned configurations outperform the baseline on the grid search datasets, we observe similar recalibration performance on the control datasets. With default parameters, the optimization problems reduce to

$$\min_{\alpha, b, v} \frac{1}{n_{\text{cal}}} \sum_{i=1}^{n_{\text{cal}}} \ell(g_{\text{SVS}}(x_i), y_i) + \frac{k}{n_{\text{cal}}} \|b\|_2^2 + \frac{k}{n_{\text{cal}}} \|v\|_2^2$$

for SVS and

$$\min_{\alpha, b, v, M} \frac{1}{n_{\text{cal}}} \sum_{i=1}^{n_{\text{cal}}} \ell(g_{\text{SMS}}(x_i), y_i) + \frac{k}{n_{\text{cal}}} \|b\|_2^2 + \frac{k}{n_{\text{cal}}} \|v\|_2^2 + \frac{k(k-1)}{n_{\text{cal}}} \|M\|_2^2$$

for SMS. We used these default hyperparameters in the following analyses for simplicity, and we report results for the entire set of 68 multiclass datasets ($\simeq 1400$ experiments).

5 Experiments

5.1 Implementation

We release Python solvers to fit vector (3) and matrix scaling (2) with our hierarchical regularization structure, for user-specified regularization hyperparameters. Our solvers implement the SAGA algorithm (Defazio et al., 2014) and we optimize execution time with just-in-time compilation using Numba (Lam et al., 2015). We make these new calibration functions available in two sklearn classifier style modules: `SVSCalibrator` and `SMSCalibrator` in our `probmetrics` package github.com/dholzmueller/probmetrics/. Usage is illustrated in Listing 1.

```

1 from probmetrics.calibrators import SMSCalibrator
2
3 p_cal = model.predict_proba(X_cal)
4
5 sms = SMSCalibrator(
6     penalty='ridge',
7     rho = 1.0,
8     tau = 1.0,
9     lambda_intercept = 1.0,
10    lambda_diagonal = 1.0,
11    lambda_off_diagonal = 1.0
12 )
13 sms.fit(p_cal, y_cal)
14
15 # Initial preds:
16 p_test = my_model.predict_proba(X_test)
17 # Calibrated preds:
18 p_test = sms.predict_proba(p_test)

```

Listing 1: Post-hoc calibration with SMS.

Existing vector and matrix scaling implementations rely on quasi-Newton solvers such as BFGS or L-BFGS, which assume differentiability. In contrast, our SAGA-based implementation supports composite objectives with non-smooth regularizers, thereby enabling logistic post-hoc calibration with a richer family of penalties. In our modules, exponents ρ and τ and group-specific coefficients λ_b , λ_v and λ_M can be set manually. The penalty used (which corresponds to the order of the norm δ) can be one of: MCP (Zhang, 2010), LASSO (Tibshirani, 1996), group LASSO (Yuan and Lin, 2006) and ridge.

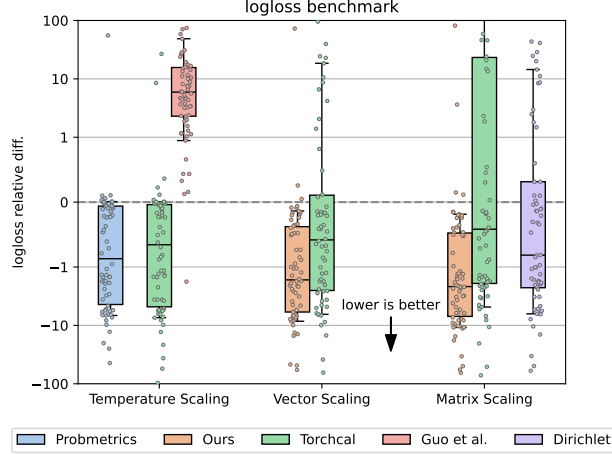


Figure 1: *Relative differences in test logloss (lower is better) after recalibration for our vector and matrix scaling functions, compared with other existing implementations.* Each dot represents the average relative loss difference obtained for one tabular dataset, over 21 experiments (7 models, 3 folds). Box-plots show the 10, 25, 50, 75, and 90% quantiles. Relative differences (y-axis) are plotted using a log scale and clipped to -100% loss (min) and +100% loss (max).

The impact of regularization in (3) and (2) is directly impacted by the scale of the logits. For smaller logits, larger changes in parameter value are needed to achieve the same effect. To make our configuration of the regularization parameters robust to more or less confident classifiers, we decide to apply SVS and SMS on logits rescaled using temperature scaling. In practice, we pre-process probabilities with the temperature scaling implementation presented in Berta et al. (2025) (using Laplace smoothing to avoid infinite temperatures when accuracy is 100%) before fitting SVS or SMS. This allows us to initialize the global scaling parameter α to one, yielding faster convergence.

Remark. *Logistic calibration functions take as input probabilities predicted by the initial model on the calibration set but operate on the logits of these predicted probabilities. In practice, computing logits from predicted probabilities needs to be implemented carefully. In our package, we first compute the log probabilities (that can contain infinite values) and then clip these to the log of the smallest normal float32 (around -90).*

5.2 Tabular Experiments

To benchmark the different multiclass post-hoc calibration methods that we introduced, we use again predictions released by Salinas and Erickson (2024). As detailed in the previous section, we have $D = 68$ multiclass datasets, $M = 7$ model configurations, and $T = 3$ classification tasks per dataset-model pair, resulting in a total of around 1400 experiments. All our experiments and figures can be reproduced using our experimental repository github.com/eugeneberta/LogisticCalibrationBenchmark.

In Figure 1 we compare our implementations (with default regularization hyperparameters) against logistic re-calibration baselines. As a general baseline, we use the torchcal package by Ranjan (2023). It uses pytorch-minimize (Feinman, 2021) to minimize the logloss after post-hoc calibration on the calibration set. For temperature scaling, we also report the original implementation by Guo et al. (2017) (the authors recently fixed a convergence issue in their implementation, which now performs better than reported), and the implementation previously presented in the probmetrics package (Berta et al., 2025). Finally, for matrix scaling, we report results obtained with Dirichlet calibration (Kull et al., 2019). In the original Dirichlet calibration paper, the authors recommend performing a grid search to select the best regularization parameters on every dataset, using cross-validation on the calibration set. Given that fitting Dirichlet calibration once on our 1400 experiments is already very slow, we fix the regularization parameters to 10^{-3} , the default value recommended in the supplementary material. Notice that Dirichlet calibration can be recovered with a certain choice of hyperparameters in our matrix scaling framework (2). Our grid search in the previous section revealed that to be suboptimal.

We compare different calibration methods in terms of test logloss after re-calibration. Logloss being a proper scoring rule Gneiting and Raftery (2007), it evaluates forecast quality, including calibration error Bröcker (2009); Kull and Flach (2015), making this a principled way to measure re-calibration performance. The same plots for Brier score can be found in Appendix D.

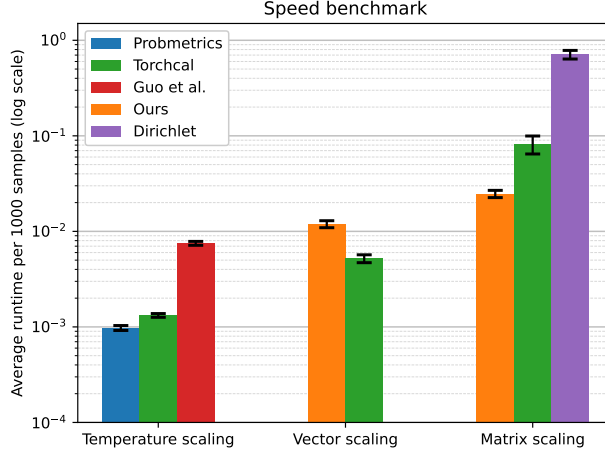


Figure 2: *Average calibration function fitting time for 1000 samples.* We compute the average using all our 1372 multiclass experiments. Error bars are computed as the standard deviation of the fitting time for every experiment (normalized for 1000 samples) divided by the square root of the number of datasets times number of models. Average runtimes (y-axis) are plotted using a log scale.

We see that baselines suffer from overfitting: for torchcal, more parametrized methods translate to more datasets with increased logloss after recalibration. Matrix scaling drastically overfits with degraded test performance on almost half the datasets. Even with regularization, Dirichlet only partially controls overfitting and underperforms standard temperature scaling or vector scaling, while being orders of magnitude slower to run.

Our hierarchical regularization structure, on the other hand, is effective at preventing overfitting and allows for consistent improvement as the number of parameters increases. Using insights from Section 2, we know that more complex recalibration functions alleviate the constraints on the logit distribution of the initial model f . In some scenarios, temperature scaling might be far from well-specified while vector and matrix scaling can help to get closer to the optimal recalibration function g^* , which explains the observed differences. We see that even for large quantiles of the loss difference distribution, matrix scaling and vector scaling do not overfit. The gains reported on the bottom of the distributions are, however, growing with the number of parameters. This demonstrates that we successfully built a post-hoc calibration method that navigates the tradeoff between under- and overfitting the calibration set, by adapting to the number of classes k and calibration points n . In Appendix D, we report similar results for the Brier score, as well as improvement plots separately for each model in our benchmark.

On the speed benchmark (Figure 2), we observe that our implementations have fitting times comparable to torchcal, despite the fact that they include regularization (note that our functions need to compile when called for the first time, which is not included in the benchmark). When compared to Dirichlet calibration, our matrix scaling implementation is more than ten times faster. Given that it is standard practice to select regularization parameters with a grid search and cross-validation (Kull et al., 2019), these time considerations can make large differences for users.

5.3 Computer Vision Experiments

To benchmark our re-calibration functions on computer vision experiments, we use logits for several deep neural network architectures trained on CIFAR-10, CIFAR-100 and ImageNet, provided by Kull et al. (2019).

In Table 1, Table 2 and Table 3 we report the absolute difference in logloss obtained after re-calibration with temperature scaling (TS probm.), torchcal's vector and matrix scaling, Dirichlet calibration as well as for our own SVS and SMS, for CIFAR-10, CIFAR-100 and ImageNet respectively. For ImageNet, there are 1000 classes, so fitting matrix scaling requires more than 10^6 parameters which is prohibitively large, hence we only report results for temperature and vector scaling for this dataset.

We see that the largest test loss improvement is always achieved by SVS or SMS, with SMS providing the best re-calibration in all cases but one. Sometimes, large improvements over temperature scaling and baselines can be achieved. For CIFAR-100, which has a large number of classes, we see that non-regularized matrix scaling (torchcal MS) has skyrocketing test loss and Dirichlet scaling's regularization fails to prevent overfitting. While SVS seems only marginally better than non-regularized vector scaling on CIFAR-10 and CIFAR-100, we see on the ImageNet

results that regularization makes a difference when the number of classes becomes very large, which could become even more striking for unbalanced datasets.

Model	TS	VS		MS		
	probm.	SVS	torchcal	SMS	torchcal	Dirichlet
densenet40	-0.206	-0.208	-0.206	-0.209	-0.203	-0.206
lenet5	-0.023	-0.073	-0.076	-0.080	-0.077	-0.076
resnet110	-0.149	-0.151	-0.150	-0.155	-0.146	-0.149
resnet110-SD	-0.128	-0.130	-0.128	-0.130	-0.116	-0.121
resnet-wide32	-0.191	-0.199	-0.199	-0.201	-0.189	-0.192

Table 1: Logloss absolute improvement on CIFAR-10

Model	TS	VS		MS		
	probm.	SVS	torchcal	SMS	torchcal	Dirichlet
densenet40	-0.961	-0.967	-0.958	-0.970	28.982	1.075
lenet5	-0.134	-0.219	-0.266	-0.273	8.204	0.166
resnet110	-0.602	-0.608	-0.598	-0.608	35.361	0.400
resnet110-SD	-0.410	-0.423	-0.421	-0.437	37.586	1.201
resnet-wide32	-0.858	-0.864	-0.851	-0.869	25.516	0.540

Table 2: Logloss absolute improvement on CIFAR-100

Model	TS	VS	
	probm.	SVS	torchcal
densenet161	-0.035	-0.037	0.007
resnet152	-0.047	-0.049	-0.015

Table 3: Logloss absolute improvement on ImageNet.

Conclusion

We have demonstrated that parametric post-hoc calibration functions based on logistic regression can be motivated theoretically for both binary and multiclass classification. This insight naturally leads to the use of more expressive calibration methods beyond standard temperature scaling, such as matrix scaling in the multiclass setting. To turn such methods into a practical tool, it is necessary to address the fundamental tradeoffs that arise when models of different complexity are used for the post-hoc calibration functions. We have shown how such tradeoffs can be addressed with novel regularization schemes. Through extensive experiments, we demonstrate that such schemes can yield substantial improvements over existing logistic-based post-hoc calibration techniques.

Our implementations, released in an open-source github package², offer significant performance gains and computational efficiency compared to existing methods. They accommodate various penalties, including MCP, LASSO, group LASSO, and ridge, with independent tuning of regularization strengths across parameter groups, offering the user the opportunity to find the best regularization parameters for every scenario. For strong out-of-the-box performance, we propose default hyperparameters that generalize well across varying numbers of classes and calibration points, and leverage meta-learning to validate this default configuration.

The empirical results consistently show that our approach yields better recalibration, with more complex models outperforming simpler ones. Our regularization scheme effectively mitigates overfitting, allowing more expressive models to capture complex miscalibration patterns without degrading generalization performance. This work highlights the importance of carefully designed regularization in unlocking the full potential of richer calibration functions, making them a compelling replacement for common temperature, vector, and matrix scaling implementations.

²github.com/dholzmueller/probmetrics/

Acknowledgements

The authors would like to thank Adrien Taylor for discussions regarding this work.

This publication is part of the Chair “Markets and Learning”, supported by Air Liquide, BNP PARIBAS ASSET MANAGEMENT Europe, EDF, Orange and SNCF, sponsors of the Inria Foundation.

This work received support from the French government, managed by the National Research Agency, under the France 2030 program with the reference “PR[AI]RIE-PSAI” (ANR-23-IACL-0008).

Funded by the European Union (ERC-2022-SYG-OCEAN-101071601). Views and opinions expressed are however those of the author(s) only and do not necessarily reflect those of the European Union or the European Research Council Executive Agency. Neither the European Union nor the granting authority can be held responsible for them.

References

Akiba, T., Sano, S., Yanase, T., Ohta, T., and Koyama, M. (2019). Optuna: A next-generation hyperparameter optimization framework. In *International Conference on Knowledge Discovery and Data Mining*.

Berta, E., Holzmüller, D., Jordan, M. I., and Bach, F. (2025). Rethinking early stopping: Refine, then calibrate. *arXiv preprint arXiv:2501.19195*.

Bishop, C. M. (2006). *Pattern Recognition and Machine Learning*. Information Science and Statistics. Springer, New York.

Böken, B. (2021). On the appropriateness of platt scaling in classifier calibration. *Information Systems*, 95:101641.

Breiman, L. (2001). Random forests. *Machine Learning*, 45(1):5–32.

Bröcker, J. (2009). Reliability, sufficiency, and the decomposition of proper scores. *Quarterly Journal of the Royal Meteorological Society: A journal of the atmospheric sciences, applied meteorology and physical oceanography*, 135(643):1512–1519.

Chen, T. and Guestrin, C. (2016). Xgboost: A scalable tree boosting system. In *International Conference on Knowledge Discovery and Data Mining*.

Defazio, A., Bach, F., and Lacoste-Julien, S. (2014). Saga: A fast incremental gradient method with support for non-strongly convex composite objectives. In *Advances in Neural Information Processing Systems*.

Erickson, N., Mueller, J., Shirkov, A., Zhang, H., Larroy, P., Li, M., and Smola, A. (2020). AutoGluon-Tabular: Robust and accurate AutoML for structured data. In *ICML Workshop on Automated Machine Learning*.

Feinman, R. (2021). Pytorch-minimize: a library for numerical optimization with autograd.

Gneiting, T. and Raftery, A. E. (2007). Strictly proper scoring rules, prediction, and estimation. *Journal of the American Statistical Association*, 102(477):359–378.

Guo, C., Pleiss, G., Sun, Y., and Weinberger, K. Q. (2017). On calibration of modern neural networks. In *International Conference on Machine Learning*.

Howard, J. and Gugger, S. (2020). Fastai: A layered API for deep learning. *Information*, 11(2).

Jordan, M. I. (1995). Why the logistic function? a tutorial discussion on probabilities and neural networks. *Computational Cognitive Science Technical Report 9503*.

Ke, G., Meng, Q., Finley, T., Wang, T., Chen, W., Ma, W., Ye, Q., and Liu, T.-Y. (2017). Lightgbm: A highly efficient gradient boosting decision tree. In *Advances in Neural Information Processing Systems*.

Kull, M., Filho, T. S., and Flach, P. (2017). Beta calibration: a well-founded and easily implemented improvement on logistic calibration for binary classifiers. In *International Conference on Artificial Intelligence and Statistics*.

Kull, M. and Flach, P. (2015). Novel decompositions of proper scoring rules for classification: Score adjustment as precursor to calibration. In *Machine Learning and Knowledge Discovery in Databases*.

Kull, M., Perello Nieto, M., Kängsepp, M., Silva Filho, T., Song, H., and Flach, P. (2019). Beyond temperature scaling: Obtaining well-calibrated multi-class probabilities with dirichlet calibration. In *Advances in Neural Information Processing Systems*.

Lam, S. K., Pitrou, A., and Seibert, S. (2015). Numba: A LLVM-based python JIT compiler. In *Second Workshop on the LLVM Compiler Infrastructure in HPC*.

Liu, D. C. and Nocedal, J. (1989). On the limited memory BFGS method for large scale optimization. *Mathematical Programming*, 45(1):503–528.

Paszke, A., Gross, S., Massa, F., Lerer, A., Bradbury, J., Chanan, G., Killeen, T., Lin, Z., Gimelshein, N., Antiga, L., et al. (2019). Pytorch: An imperative style, high-performance deep learning library. In *Advances in Neural Information Processing Systems*.

Prokhorenkova, L., Gusev, G., Vorobev, A., Dorogush, A. V., and Gulin, A. (2018). CatBoost: unbiased boosting with categorical features. In *Advances in Neural Information Processing Systems*.

Ranjan, R. (2023). torchcal: post-hoc calibration on GPU.

Salinas, D. and Erickson, N. (2024). Tabrepo: A large scale repository of tabular model evaluations and its autoML applications. In *AutoML Conference 2024 (ABCD Track)*.

Tibshirani, R. (1996). Regression shrinkage and selection via the lasso. *Journal of the Royal Statistical Society Series B: Statistical Methodology*, 58(1):267–288.

Vanschoren, J. (2018). Meta-learning: A survey. *arXiv preprint arXiv:1810.03548*.

Yuan, M. and Lin, Y. (2006). Model selection and estimation in regression with grouped variables. *Journal of the Royal Statistical Society Series B: Statistical Methodology*, 68(1):49–67.

Zadrozny, B. and Elkan, C. (2002). Transforming classifier scores into accurate multiclass probability estimates. In *International Conference on Knowledge Discovery and Data Mining*.

Zhang, C.-H. (2010). Nearly unbiased variable selection under minimax concave penalty. *The Annals of Statistics*, 38(2):894–942.

Appendices

A Binary Logistic Calibration

In the binary classification setting, we observe some random variable $X \in \mathcal{X}$ and try to predict the value of some other (binary) random variable $Y \in \{+1, -1\}$, traditionally known as the *outcome*. Statistical models typically make continuous predictions $p \in [0, 1]$, where larger p indicates larger certainty from the model that the outcome is $Y = +1$. In the following we denote σ the sigmoid function $\sigma(x) = \frac{1}{1+\exp(-x)}$ and σ^{-1} its inverse, the logit function $\sigma^{-1}(x) = \log \frac{x}{1-x}$. $\mathbb{S}_+^{d \times d}$ is the space of $d \times d$ positive semidefinite matrices.

A.1 Motivating Calibration with Logistic Regression

Many existing binary parametric post-hoc calibration methods derive from logistic regression on the log odds $\sigma^{-1}(p) = \log \frac{p}{1-p}$ of the predicted probabilities $f(X) = p$. We will see that this choice can be motivated from a simple setting.

Assume $\mathcal{X} = \mathbb{R}^d$, and consider a binary class-conditional Gaussian data model $\mathbb{P}(X | Y = +1) = \mathcal{N}(\mu_+, \Sigma_+)$ and $\mathbb{P}(X | Y = -1) = \mathcal{N}(\mu_-, \Sigma_-)$ with mean vectors $\mu_+, \mu_- \in \mathbb{R}^d$, and covariance matrices $\Sigma_+, \Sigma_- \in \mathbb{S}_+^{d \times d}$. We denote the class probabilities $\pi_+ = \mathbb{P}(Y = +1)$ and $\pi_- = \mathbb{P}(Y = -1)$. Let f be a logistic regression classifier parametrized by some weight vector $w \in \mathbb{R}^d$: $f(X) = \sigma(w^\top X)$. We have that the logits $w^\top X$ conditioned on each class follow a one-dimensional Gaussian distribution:

$$\mathbb{P}(w^\top X | Y = +1) = \mathcal{N}(w^\top \mu_+, w^\top \Sigma_+ w), \quad \mathbb{P}(w^\top X | Y = -1) = \mathcal{N}(w^\top \mu_-, w^\top \Sigma_- w).$$

Denoting the means $m_+ := w^\top \mu_+$, $m_- := w^\top \mu_-$ and variances $\sigma_+^2 := w^\top \Sigma_+ w$, $\sigma_-^2 := w^\top \Sigma_- w$ we have that

$$\mathbb{P}(Y = +1 | w^\top X = x) = \sigma(ax^2 + bx + c),$$

with

$$a = \frac{1}{2\sigma_-^2} - \frac{1}{2\sigma_+^2}, \quad b = \frac{m_+}{\sigma_+^2} - \frac{m_-}{\sigma_-^2}, \quad c = \log\left(\frac{\pi_+ \sigma_-}{\pi_- \sigma_+}\right) + \frac{m_-^2}{2\sigma_-^2} - \frac{m_+^2}{2\sigma_+^2}.$$

See Appendix B for a proof. We want our classifier f to be calibrated, that is

$$\mathbb{P}(Y = +1 | f(X) = s) = s.$$

In our example, $f(X) = s \iff \sigma(w^\top X) = s \iff w^\top X = \sigma^{-1}(s)$. So the distribution of Y is

$$\mathbb{P}(Y = +1 | f(X) = s) = \sigma(a\sigma^{-1}(s)^2 + b\sigma^{-1}(s) + c).$$

Denoting g the post-hoc calibration function $g(s) = \sigma(a\sigma^{-1}(s)^2 + b\sigma^{-1}(s) + c)$, it holds that $\mathbb{P}(Y = +1 | f(X) = s) = g(s)$. In general, the function g does not have to be an injection; for a given value $g \circ f = p$ we define the set $S_p = \{s | g(s) = p\}$, then

$$\begin{aligned} \mathbb{P}(Y = +1 | g \circ f(X) = p) &= \int_{S_p} \mathbb{P}(Y = +1 | f(X) = s) \mathbb{P}(f(X) = s | g \circ f(X) = p) ds \\ &= \int_{S_p} p \mathbb{P}(f(X) = s | g \circ f(X) = p) ds \\ &= p, \end{aligned}$$

which proves that $g \circ f$ is calibrated.

Remark. In our motivating example, the logistic calibration function is well specified because the class-conditional logit distributions are Gaussian. However, performing post-hoc calibration with logistic regression does not correspond to assuming that the class-conditional distributions are Gaussian as it is sometimes suggested in the literature. There is a wide range of distribution pairs for which the conditional is logistic, as discussed in Jordan (1995) and Böken (2021). It holds as soon as logistic regression is well specified, see (Bishop, 2006).

A.2 Logistic Calibration Functions

Our example setting in Appendix A.1 motivated the use of a logistic model as a post-hoc calibration function. In practice however, we cannot compute coefficients a , b and c directly. For a real world dataset, the data is not normally distributed and our classifier does not have to be logistic regression so logistic re-calibration might not be well specified. We hope there exists some parameters of g for which $g \circ f$ is approximately calibrated. We resort to empirical risk minimization to find such coefficients. Using the reserved calibration set $(x_i, y_i)_{1 \leq i \leq n_{\text{cal}}}$, we solve

$$\min_g \frac{1}{n_{\text{cal}}} \sum_{i=1}^{n_{\text{cal}}} \ell(g \circ f(x_i), y_i), \quad (4)$$

where g is parametrized by the coefficients of the logistic model. ℓ is typically the logloss, which makes the problem convex and thus allows us to find the optimal coefficients easily.

In the literature, different choices for the function g based on the logistic model coexist:

- Linear scaling (known as temperature scaling (Guo et al., 2017)): $g(x) = \sigma(\alpha\sigma^{-1}(x))$, g is parametrized only by a linear coefficient α .
- Affine scaling (known as Beta scaling (Kull et al., 2017)): $g(x) = \sigma(\alpha\sigma^{-1}(x) + \beta)$, g is parametrized by both a linear and constant coefficient α and β .
- To the best of our knowledge, quadratic scaling: $g(x) = \sigma(\gamma\sigma^{-1}(x)^2 + \alpha\sigma^{-1}(x) + \beta)$, has not been used for post-hoc calibration before. We include it in our experiments.

In the binary case, we only have 1, 2 or 3 parameters (respectively for linear, affine and quadratic scaling) to learn, so the risk of overfitting the empirical risk estimate is limited. We evaluate our three methods without regularization, although our implementation can accommodate different penalties on any of the three parameters. Before moving to empirical results, we look back at our example from Appendix A.1 to get some insight about the different design choices for g .

The affine hypothesis. Looking back at our data model, the affine hypothesis corresponds to setting $a = 0$, which implies $\sigma_- = \sigma_+$. In other words, affine scaling is well specified only when the two class-wise logit distributions have the same variance. We have no guarantee that this should hold in practice, suggesting that quadratic scaling might bring further improvement over affine scaling in scenarios where this assumption is not satisfied.

The linear hypothesis. The linear hypothesis is even more constraining. Setting $c = 0$ puts constraints on the means, variances, but also class probabilities π_+ and π_- . We see no reason why this should be true in practice and we thus expect to see a large performance gap between linear and affine scaling.

A.3 Experiments

A.3.1 Implementation

For linear, affine and quadratic scaling, we provide efficient Python implementations that solve the convex optimization problem (4). We use the default sklearn implementation for logistic regression, that uses L-BFGS Liu and Nocedal (1989) and we remove regularization. Depending on whether we want to apply linear, affine or quadratic scaling, we feed only logits $(\sigma^{-1}(p_i))_{1 \leq i \leq n_{\text{cal}}}$, a constant and logits $(1, \sigma^{-1}(p_i))_{1 \leq i \leq n_{\text{cal}}}$ or a constant, logits and squared logits $(1, \sigma^{-1}(p_i), \sigma^{-1}(p_i)^2)_{1 \leq i \leq n_{\text{cal}}}$ to the classifier. We package this into a calibration module `BinaryLogisticCalibrator` in `probmetrics` (github.com/dholzmueller/probmetrics/). For ease of use, we follow the sklearn classifier format as illustrated in Listing 2.

```

1 from probmetrics.calibrators import BinaryLogisticCalibrator
2
3 cal = BinaryLogisticCalibrator(type='quadratic')
4 cal.fit(p_val, y_val)
5
6 calibrated_preds = cal.predict_proba(p_test)

```

Listing 2: Post-hoc calibration with probmetric's binary calibrator.

We also release SAGA-based implementation for the three methods (Defazio et al., 2014), with execution time optimized using just-in-time compilation with Numba (Lam et al., 2015). Since SAGA can accommodate non smooth

penalties, these are compatible with: MCP (Zhang, 2010), LASSO (Tibshirani, 1996) and ridge, should the user want to apply regularization on the intercept and/or quadratic parameters for affine scaling and quadratic scaling. We refer to our package for details on the implementation, regularization options and running examples.

A.3.2 Tabular Experiments

To benchmark the different binary calibration methods that we reviewed, we use TabRepo, a large set of model predictions provided by Salinas and Erickson (2024). TabRepo stores predictions obtained by training classical machine learning and deep learning models on dozens of tabular datasets for a variety of hyperparameter configurations. We use the predictions of $M = 7$ different models (logistic regression, CatBoost (Prokhorenkova et al., 2018), LightGBM (Ke et al., 2017), XGBoost (Chen and Guestrin, 2016), random forest (Breiman, 2001), a pytorch neural net (Paszke et al., 2019) and a FastAI neural net Howard and Gugger (2020)) on the $D = 105$ binary datasets available. For each dataset, the data is split in 10 folds, and $T = 3$ separate tasks are created by using one of the first three folds as a test set. For each of the tasks, the remaining data is used for eight-fold cross-validation, and the predictions of the eight models on their respective validation folds are concatenated and provided as a validation set, that we use to fit post-hoc calibration models. This results in a total of $M \times D \times T \simeq 2200$ experiments that we use to benchmark our calibration techniques. Each model is fitted using the training data and early stopping is performed based the validation logloss (except for linear regression and random forest, for which no early stopping is required). For every experiment, predictions are available for the model trained with default hyperparameters as well as for 200 randomly generated hyperparameter configurations. We evaluate our post-hoc calibration functions on the models trained with the hyperparameter configuration that achieves the smallest validation error (*tuned configuration*). We fit our post-hoc calibration functions using the validation data as explained above and report the gains obtained on the test set. All our experiments and figures can be reproduced using our experimental repository github.com/eugeneberta/LogisticCalibrationBenchmark.

Remark. *For data-efficiency, we reuse the validation set to fit the post-hoc calibration function. Note that it is already used for early stopping (except for logistic regression and random forest) and, for tuned configurations, to select the best hyperparameter configuration. We acknowledge this deviation from standard protocol could risk overfitting. However, our empirical results on the test set demonstrate substantial improvements from recalibration, suggesting that generalization was not compromised.*

In Figure A.1 we compare our implementations against logistic re-calibration baselines. We compare linear scaling with existing temperature scaling implementations: the original implementation by Guo et al. (2017), and an implementation previously presented in the probmetrics package (Berta et al., 2025). For affine and quadratic scaling, we report the performance of our implementation.

We report the average change in test logloss observed after post-hoc calibration, with lower values indicating better recalibration. The original temperature scaling implementation by Guo et al. (2017) does not always converge and is thus largely suboptimal (the authors recently fixed a convergence issue in their implementation, which now performs better than reported). The difference between probmetrics' TS and ours comes from the fact that probmetrics uses Laplace smoothing on the predicted probabilities. As expected, affine scaling yields a noticeable improvement over standard linear scaling. Interestingly, we observe additional gains for quadratic scaling over affine scaling. On our large scale benchmark, this method, that has not been introduced previously in the literature, performs best. In Appendix C, we plot the results obtained for Brier score (as well as improvement plots separately for each model in our benchmark), that lead to the same conclusions.

On Figure A.2 we plot the average fitting time per 1000 samples for the different binary calibration functions in our benchmark. Our implementation is the fastest available for linear (temperature) scaling. Affine and quadratic scaling are slower but still converge in reasonable time. These runtime considerations can be crucial when post-hoc calibration is performed repeatedly, for example when estimating refinement for early stopping (Berta et al., 2025).

Remark. *Logistic calibration functions take as input probabilities predicted by the initial model on the calibration set but operate on the logits of these predicted probabilities. The binary logit function that maps predicted probabilities to logits $\sigma^{-1}(p) = \log \frac{p}{1-p}$ needs to be implemented carefully in practice. In our package, to compute binary logits, we first compute $\log(p) - \log(1-p)$ (using the numerically stable `log1p` function). This potentially returns infinite values, so we clip the outcome to minus and plus the log of the smallest float32 (around ± 90).*

B Proofs

Proof in the Binary Case. Denoting $m_+ := w^\top \mu_+$, $m_- := w^\top \mu_-$ and $\sigma_+^2 := w^\top \Sigma_+ w$, $\sigma_-^2 := w^\top \Sigma_- w$, we have

$$\mathbb{P}(w^\top X = x \mid Y = +1) = \mathcal{N}(x \mid m_+, \sigma_+^2), \quad \mathbb{P}(w^\top X = x \mid Y = -1) = \mathcal{N}(x \mid m_-, \sigma_-^2).$$

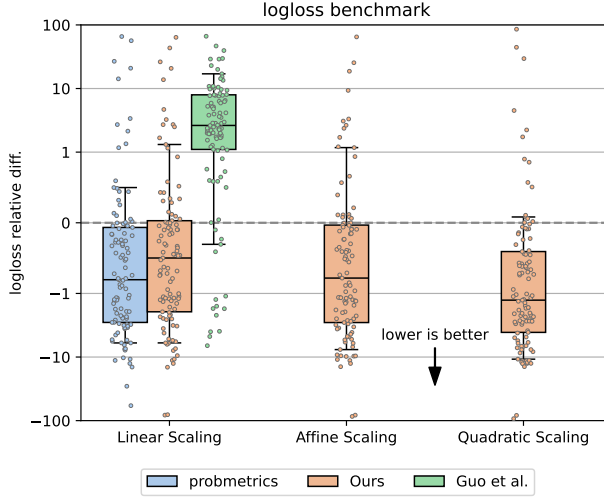


Figure A.1: *Relative differences in test logloss (lower is better) after recalibration for our linear, affine and quadratic scaling functions, compared with other existing implementations.* Each dot represents the average relative loss difference obtained for one tabular dataset, over 21 experiments (7 models, 3 folds). Box-plots show the 10, 25, 50, 75, and 90% quantiles. Relative differences (y-axis) are plotted using a log scale and clipped to -100% loss (min) and +100% loss (max).

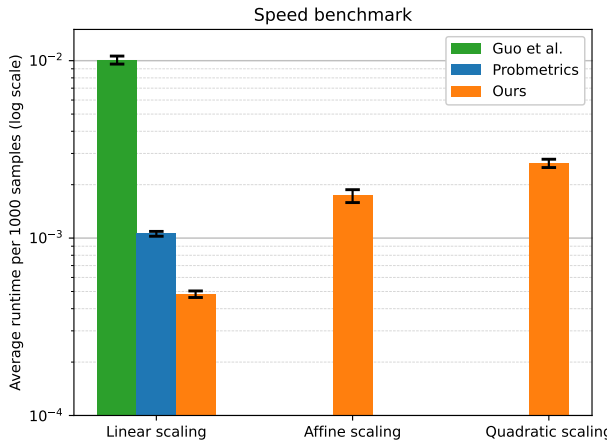


Figure A.2: *Average calibration function fitting time for 1000 samples.* We compute the average using all our 2205 binary experiments. Error bars are computed as the standard deviation of the fitting time for every experiment (normalized for 1000 samples) divided by the square root of the number of datasets times number of models. Average runtimes (y-axis) are plotted using a log scale.

Let us prove that

$$\mathbb{P}(Y = +1 \mid w^\top X = x) = \sigma(ax^2 + bx + c),$$

with

$$a = \frac{1}{2\sigma_-^2} - \frac{1}{2\sigma_+^2}, \quad b = \frac{m_+}{\sigma_+^2} - \frac{m_-}{\sigma_-^2}, \quad c = \log\left(\frac{\pi_+\sigma_-}{\pi_-\sigma_+}\right) + \frac{m_-^2}{2\sigma_-^2} - \frac{m_+^2}{2\sigma_+^2}.$$

Using Bayes' theorem,

$$\begin{aligned} \mathbb{P}(Y = +1 \mid w^\top X = x) &= \frac{\mathbb{P}(w^\top X = x \mid Y = +1)\mathbb{P}(Y = +1)}{\mathbb{P}(w^\top X = x)} \\ &= \frac{\mathbb{P}(w^\top X = x \mid Y = +1)\mathbb{P}(Y = +1)}{\mathbb{P}(w^\top X = x \mid Y = +1)\mathbb{P}(Y = +1) + \mathbb{P}(w^\top X = x \mid Y = -1)\mathbb{P}(Y = -1)} \\ &= \frac{\mathcal{N}(x \mid m_+, \sigma_+^2)\pi_+}{\mathcal{N}(x \mid m_+, \sigma_+^2)\pi_+ + \mathcal{N}(x \mid m_-, \sigma_-^2)\pi_-} \\ &= \frac{1}{1 + \frac{\pi_-}{\pi_+} \frac{\mathcal{N}(x \mid m_-, \sigma_-^2)}{\mathcal{N}(x \mid m_+, \sigma_+^2)}} \\ &= \frac{1}{1 + \frac{\pi_- \sigma_+}{\pi_+ \sigma_-} \exp\left(-\frac{(x - m_-)^2}{2\sigma_-^2} + \frac{(x - m_+)^2}{2\sigma_+^2}\right)} \\ &= \sigma\left(\frac{(x - m_-)^2}{2\sigma_-^2} - \frac{(x - m_+)^2}{2\sigma_+^2} + \log\frac{\pi_+\sigma_-}{\pi_-\sigma_+}\right) \\ &= \sigma\left(\left(\frac{1}{2\sigma_-^2} - \frac{1}{2\sigma_+^2}\right)x^2 + \left(\frac{m_+}{\sigma_+^2} - \frac{m_-}{\sigma_-^2}\right)x + \left(\frac{m_-^2}{2\sigma_-^2} - \frac{m_+^2}{2\sigma_+^2} + \log\frac{\pi_+\sigma_-}{\pi_-\sigma_+}\right)\right) \\ &= \sigma(ax^2 + bx + c), \end{aligned}$$

which concludes the proof.

Proof in the Multiclass Case. Denoting $m_i := C_k W \mu_i$, $\sigma_i := C_k W \Sigma_i W^\top C_k^\top$ and $\mathbb{P}(Y = i) = \pi_i$ for all $i \in \{0, \dots, k\}$, we have

$$\mathbb{P}(C_k W X = x \mid Y = i) = \frac{\exp\left(-\frac{1}{2}(x - m_i)^\top \sigma_i^+ (x - m_i)\right)}{\sqrt{|2\pi\sigma_i|_+}}.$$

Let us prove that

$$\mathbb{P}(Y \mid C_k W X = x) = S(x^\top \mathbf{A}x + Bx + C),$$

with \mathbf{A} a tensor in $\mathbb{R}^{k \times k \times k}$ defined by $\mathbf{A}[i, :, :] = -\frac{1}{2}\sigma_i^+$ so that $(x^\top \mathbf{A}x)_i = -\frac{1}{2}x^\top \sigma_i^+ x$, B a matrix in $\mathbb{R}^{k \times k}$ defined by $B_i = m_i^\top \sigma_i^+$ and C a vector in \mathbb{R}^k defined by $C_i = -\frac{1}{2}m_i^\top \sigma_i^+ m_i + \log(\pi_i |\sigma_i|_+^{-1/2})$.

Using Bayes' theorem,

$$\begin{aligned} \mathbb{P}(Y = i \mid C_k W X = x) &= \frac{\mathbb{P}(C_k W X = x \mid Y = i)\mathbb{P}(Y = i)}{\mathbb{P}(C_k W X = x)} \\ &= \frac{\mathbb{P}(C_k W X = x \mid Y = i)\mathbb{P}(Y = i)}{\sum_{j=1}^k \mathbb{P}(C_k W X = x \mid Y = j)\mathbb{P}(Y = j)} \\ &= \frac{\pi_i |\sigma_i|_+^{-1/2} \exp\left(-\frac{1}{2}(x - m_i)^\top \sigma_i^+ (x - m_i)\right)}{\sum_{j=1}^k \pi_j |\sigma_j|_+^{-1/2} \exp\left(-\frac{1}{2}(x - m_j)^\top \sigma_j^+ (x - m_j)\right)} \\ &= \frac{\exp\left(-\frac{1}{2}(x - m_i)^\top \sigma_i^+ (x - m_i) + \log(\pi_i |\sigma_i|_+^{-1/2})\right)}{\sum_{j=1}^k \exp\left(-\frac{1}{2}(x - m_j)^\top \sigma_j^+ (x - m_j) + \log(\pi_j |\sigma_j|_+^{-1/2})\right)} \\ &= S(x^\top \mathbf{A}x + Bx + C)_i, \end{aligned}$$

which concludes the proof.

C Additional Binary Results

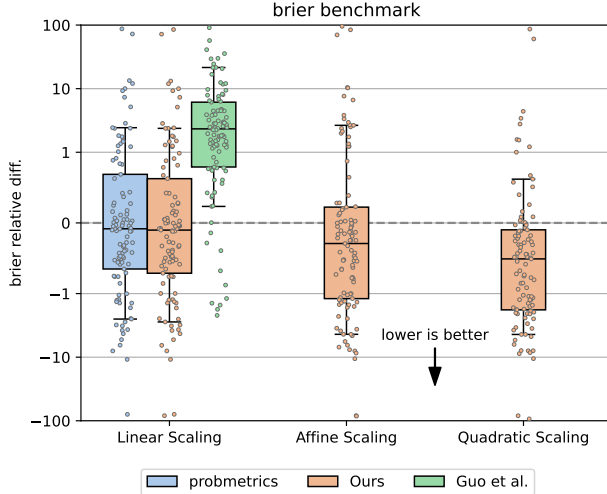


Figure C.1: *Relative differences in test Brier score (lower is better) after recalibration for our linear, affine and quadratic scaling functions, compared with other existing implementations.* Each dot represents the average relative loss difference obtained for one tabular dataset, over 21 experiments (7 models, 3 folds). Box-plots show the 10, 25, 50, 75, and 90% quantiles. Relative differences (y-axis) are plotted using a log scale and clipped to -100% loss (min) and +100% loss (max).

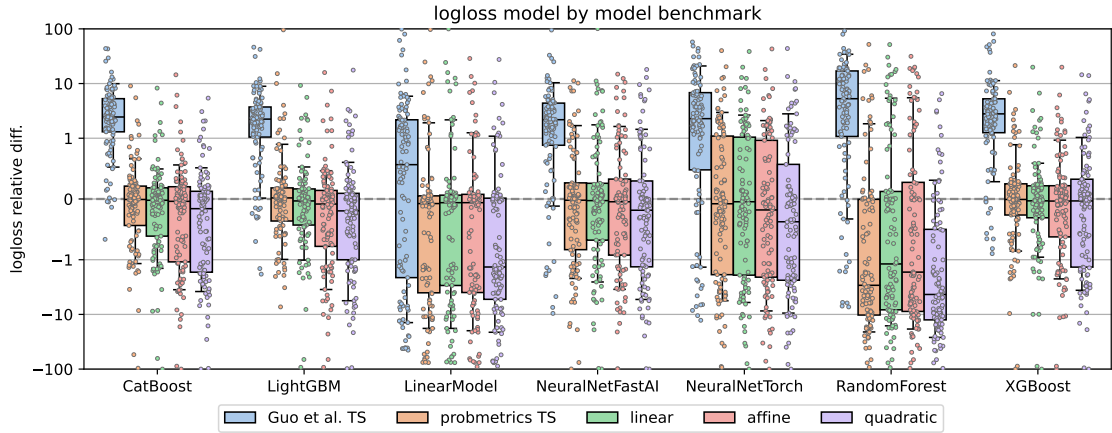


Figure C.2: *Relative differences in test logloss (lower is better) after recalibration for our linear, affine and quadratic scaling functions, compared with other existing implementations, separately for every model in our benchmark.* Each dot represents the average relative loss difference obtained for one model on one tabular dataset, over 3 folds. Box-plots show the 10, 25, 50, 75, and 90% quantiles. Relative differences (y-axis) are plotted using a log scale and clipped to -100% loss (min) and +100% loss (max).

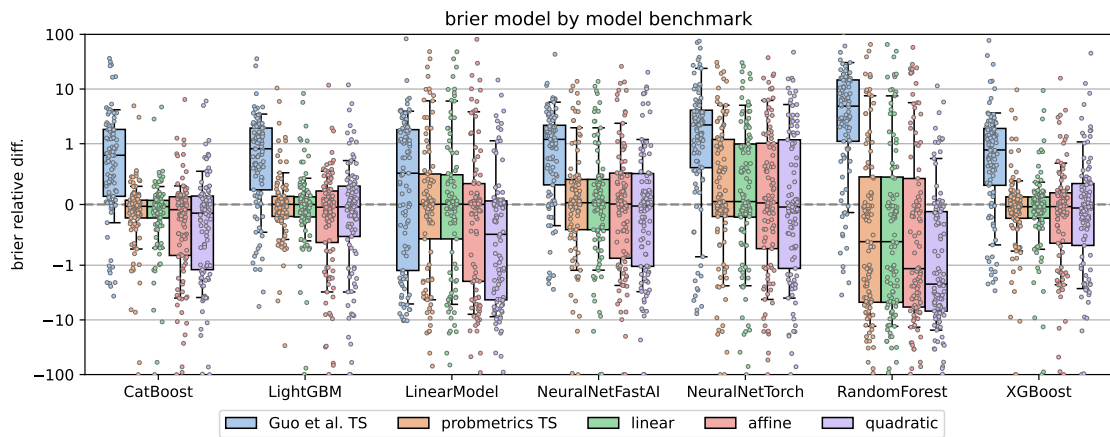


Figure C.3: *Relative differences in test Brier score (lower is better) after recalibration for our linear, affine and quadratic scaling functions, compared with other existing implementations, separately for every model in our benchmark.* Each dot represents the average relative score difference obtained for one model on one tabular dataset, over 3 folds. Box-plots show the 10, 25, 50, 75, and 90% quantiles. Relative differences (y-axis) are plotted using a log scale and clipped to -100% loss (min) and +100% loss (max).

D Additional Multiclass Results

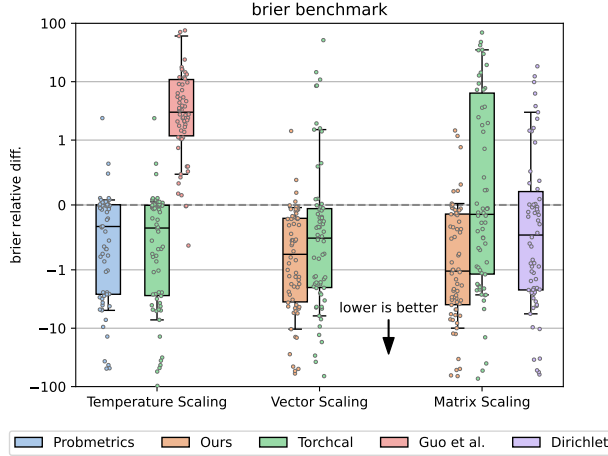


Figure D.1: *Relative differences in test Brier score (lower is better) after recalibration for our vector and matrix scaling functions, compared with other existing implementations.* Each dot represents the average relative score difference obtained for one tabular dataset, over 21 experiments (7 models, 3 folds). Box-plots show the 10, 25, 50, 75, and 90% quantiles. Relative differences (y-axis) are plotted using a log scale and clipped to -100% loss (min) and +100% loss (max).

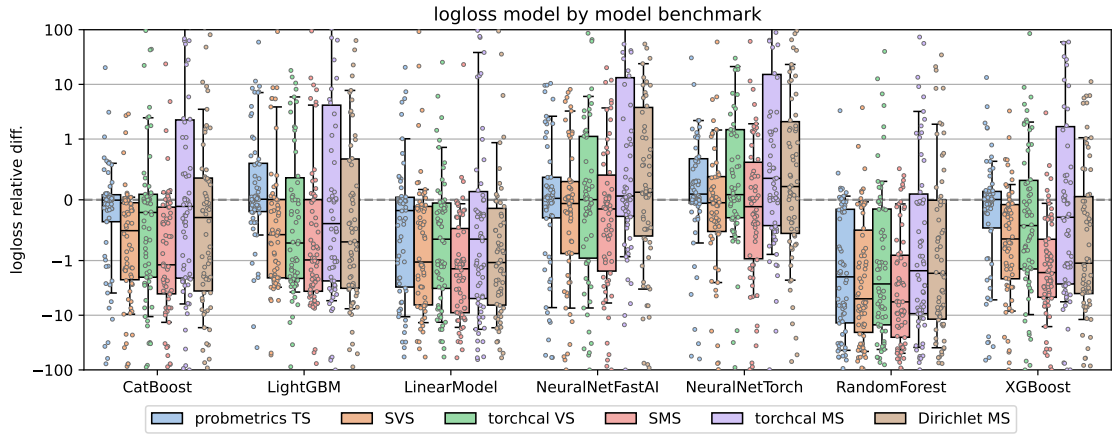


Figure D.2: *Relative differences in test logloss (lower is better) after recalibration for our vector and matrix scaling functions, compared with other existing implementations, separately for every model in our benchmark.* Each dot represents the average relative loss difference obtained for one model on one tabular dataset, over 3 folds. Box-plots show the 10, 25, 50, 75, and 90% quantiles. Relative differences (y-axis) are plotted using a log scale and clipped to -100% loss (min) and +100% loss (max).

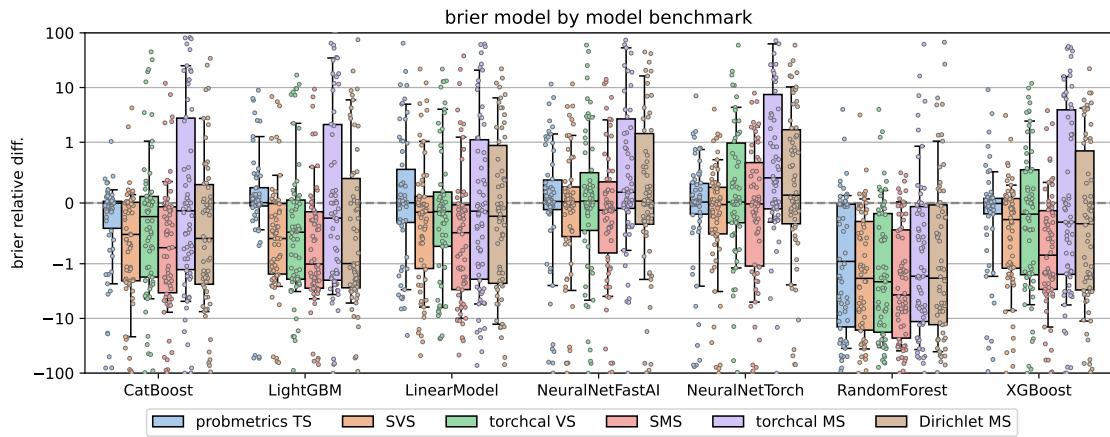


Figure D.3: *Relative differences in test Brier score (lower is better) after recalibration for our vector and matrix scaling functions, compared with other existing implementations, separately for every model in our benchmark.* Each dot represents the average relative score difference obtained for one model on one tabular dataset, over 3 folds. Box-plots show the 10, 25, 50, 75, and 90% quantiles. Relative differences (y-axis) are plotted using a log scale and clipped to -100% loss (min) and +100% loss (max).